

Lab - Mechatronics
Modelling and control of a Magnetic Levitation System

Tommaso Bocchietti 10740309
Daniele Cianca 000000000
Sara Orazio 000000000

A.Y. 2024/25



POLITECNICO
MILANO 1863

Contents

1	Introduction	3
2	Magnetic Levitation System	4
2.1	Model derivation	5
2.1.1	Mathematical model	5
2.1.2	Black zone control	7
2.1.3	Literature model	7
2.2	Model Linearization	8
2.3	State Space Representation	8
2.4	Parameters identification	9
3	Controller Design	12
3.1	PID Controller	13
3.1.1	Simple PID	13
3.1.2	PID with Anti-Windup correction	13
3.1.3	Bla bla bla	13
3.2	Cascaded Controller	14
3.3	Pole Placement Controller	15
3.4	LQR Controller	16
3.5	MPC Controller	17
3.6	Adaptive Control	18
3.7	Backstepping	19
3.8	Feedback Linearization	20
4	Controllers Comparison	21
5	Conclusions	22

List of Figures

1	Magnetic Levitation System	4
2	Schematic representation of the upper half of the MLS system.	4
3	Schematic representation of the MLS system and description of the components.	5
4	RL circuit identification	10
5	Levitation current	10
6	Dynamic inductance characteristics	11

List of Tables

1	Parameters to be identified	9
2	Directly measured parameters	9
3	RL circuit identification parameters	10
4	Dynamic inductance characteristics	11
5	Controllers assignment	12

Listings

1 Introduction

The aim of this laboratory experience is to precisely control the levitation of a ferromagnetic object immerse in a magnetic field. This kind of system is commonly referred to as a Magnetic Levitation System (MLS).

The work has been splitted into two main phases:

- **Modelling and parameters identification:** in this phase, the system has been modelled by means of both differential equations and state space representation, and the parameters of the model have been identified through experimental data performed directly on the real system. Some preliminary consideration about stability and controllability have also been made.
- **Control design:** in this phase, many different control techniques have been implemented and tested. The main goal was to compare the performances of different controllers in terms of stability, robustness and tracking capabilities.

Report structure This report covers all the aspects of the laboratory experience, from the theoretical background to the practical implementation of the control algorithms. In particular, in Section 2 the system is described in detail, a model is derived and the parameters are identified. In Section ?? a set of SISO controllers are designed to work on a reduced model of the system, where only one coil is active. On the other hand, in Section ?? a set of MISO controllers are designed to work on the full model of the system, where both coils are actively used to control the position of the magnet. In Section ?? the performances of the different controllers are compared, and finally in Section 5 some conclusions are drawn.

Tools An extensive use of **MATLAB** and **Simulink** has been made to implement the controllers and to simulate the system. All the source code and simulations used for this report can be found on the GitHub repository at the following link: <https://github.com/Bocchio01/062020-Lab-Mechatronics>.

2 Magnetic Levitation System

As stated in the introduction, the system under study is the Magnetic Levitation System (MLS) provided by Inteco (producer website: <https://www.inteco.com.pl/products/magnetic-levitation-systems/>). In Figure 1 the system used in this work is shown.



Figure 1: Magnetic Levitation System

As it can be seen quite clearly, the system is composed of a simple mechanical structure that is used to support two electromagnets and an optical infrared sensor. Along with the mechanical structure, a ferromagnetic ball and a control unit are present.

At its core principle, the system uses the interaction between the magnetic field generated by the electromagnets and the ferromagnetic ball to keep the ball in a desired position. The optical sensor is used to measure the position of the ball and provide feedback to the control unit that, in turn, adjusts the voltage applied to (and indeed the current flowing through) the electromagnets to keep the ball in a desired position. In Figure 2 a schematic representation of the upper half of the system is shown.

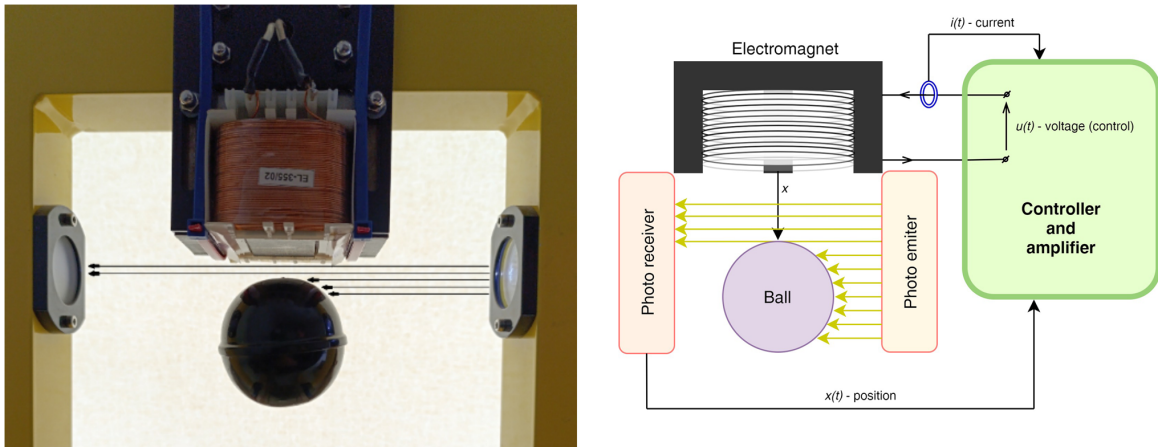


Figure 2: Schematic representation of the upper half of the MLS system.

Real world application Despite the fact that our system is a simplified use case, the magnetic levitation principle is used in many real-world applications.

One of the most common applications is the magnetic levitation trains, also known as ‘MagLev’ trains. These trains use the magnetic levitation principle to lift the train off the tracks and propel it forward using the magnetic

field generated by the tracks. The main advantage of this technology is the absence of friction between the train and the tracks, which allows the train to reach higher speeds and reduce the noise characteristic of the traditional trains. Some of the fastest (operating) trains in the world are MagLev trains, with the Shanghai MagLev train being the fastest, reaching a top speed of 623km/h [1].

Another application of the magnetic levitation principle is the magnetic bearings. These bearings use the magnetic field generated by electromagnets to levitate a rotor and keep it in a desired position. The main advantage of this technology is the absence of mechanical contact between the rotor and the stator, which allows the rotor to reach higher speeds and reduce the wear of the components.

2.1 Model derivation

The MLS is a complex system that can be divided into two main subsystems:

- **Electromagnetic subsystem:** it takes into account the electrical components of the system from the power supply to the generation of the magnetic field by the coils;
- **Mechanical subsystem:** it takes into account the dynamics of the ball and all the forces acting on it, including the electromagnetic forces generated by the magnetic field.

Due to the presence of the ball that moves inside a magnetic field, a complex connection between the two subsystems that goes beyond the simple force balance exists. For this reason, it's almost impossible to derive a complete model without considering both subsystems at the same time.

In Figure 3, a schematic representation of all the components and forces acting on the system is shown. Instead, in Table 3 a brief description of the components of the system and their units is reported.

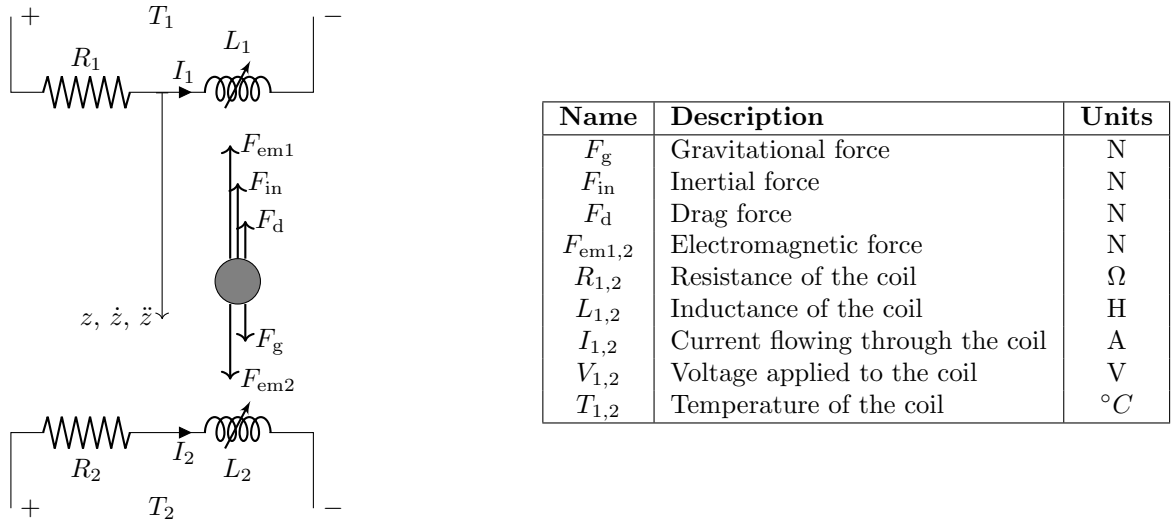


Figure 3: Schematic representation of the MLS system and description of the components.

In the following sections, we will derive the equations that governs the MLS system, adopting an energetic approach that starts from the energy conservation principle.

2.1.1 Mathematical model

We can now proceed with the derivation of the equations that govern the system.

At first, we can recall that the energy conservation principle states that the sum of the kinetic, potential, and dissipated energy of the system is equivalent to the work done by the external forces acting on the system.

Lagrange's equation Thanks to the Lagrange's equation we write the following, that encapsulates the energy conservation principle:

$$\frac{d}{dt} \left(\frac{\partial \mathcal{T}}{\partial \dot{\mathbf{u}}} \right) - \frac{\partial \mathcal{T}}{\partial \mathbf{u}} + \frac{\partial \mathcal{D}}{\partial \dot{\mathbf{u}}} + \frac{\partial \mathcal{U}}{\partial \mathbf{u}} = \mathcal{Q} \quad (1)$$

Where \mathbf{u} is the generalized coordinates of the system, \mathcal{T} is the kinetic energy of the system, \mathcal{D} is the dissipated energy of the system, \mathcal{U} is the potential energy of the system, and \mathcal{Q} is the generalized input to the system.

At first, we can give a definition of all the energetic terms included in Equation 1 for the MLS system. Notice that with respect to traditional purely mechanical systems, we also have to consider the stored energy in the coils as inductors, the dissipation due to the resistance of the coils, and the potential energy given by the external power supply.

By doing so, we can write the kinetic energy of the system as:

$$\mathcal{T} = \frac{1}{2}m\dot{z}^2 + \frac{1}{2}L_1(z, \dot{q}_1, T_1)\dot{q}_1^2 + \frac{1}{2}L_2(z, \dot{q}_2, T_2)\dot{q}_2^2 \quad (2)$$

Where m is the mass of the ball, L_1 and L_2 are the inductances of the coils, and q_1 and q_2 are the charges stored in the coils. It follows that \dot{q}_1 and \dot{q}_2 are the currents flowing through the coils.

The dissipated energy of the system can be written as:

$$\mathcal{D} = \int_{\dot{z}(\cdot)} \frac{1}{2}C_d A \rho \dot{z}^2 d\dot{z} + \int_{\dot{q}_1(\cdot)} R_1(\dot{q}_1, T_1)\dot{q}_1 d\dot{q}_1 + \int_{\dot{q}_2(\cdot)} R_2(\dot{q}_2, T_2)\dot{q}_2 d\dot{q}_2 \quad (3)$$

Where C_d is the drag coefficient, A is the cross-sectional area of the ball, and ρ is the density of the air.

Instead, the potential energy of the system can be written as:

$$\mathcal{U} = -mgz - q_1 V_1 - q_2 V_2 \quad (4)$$

Where V_1 and V_2 are the voltages applied to the coils.

Finally, the generalized input to the system can be evaluated as:

$$\mathcal{Q} = 0 \quad (5)$$

For convenience, we have chosen to consider both the external power supplied to the coils and the gravitational force as potential energy terms and not as generalized inputs. Notice also the minus sign in the gravitational potential energy term, which is due to the fact that the gravitational force increases the potential energy with respect to the chosen reference frame (positive downwards).

Electrical components model Complete also with the assumption of current independence for both the elements.

Before proceeding, it's necessary to explicitly the dependence of the inductance and resistance terms on both the currents inside the coils and the temperature of the coils.

However, we can assume that in first approximation the sensitivity of both the electrical components to the temperature is negligible. This is strong and possibly incorrect assumption, but it allows us to simplify the model and focus on the main dynamics of the system.

For the assumption stated above, we can write the resistance terms as:

$$\begin{aligned} R_1 &= R_1(\dot{q}_1, T_1) = R_{10} \\ R_2 &= R_2(\dot{q}_2, T_2) = R_{20} \end{aligned} \quad (6)$$

Where R_{*0} are the resistances of the coils at ambient temperature with negligible current flowing through them. Instead, we can write the inductance terms as:

$$\begin{aligned} L_1 &= L_1(z, \dot{q}_1, T_1) = L_{10} + L_{1z}e^{-a_1 z} \\ L_2 &= L_2(z, \dot{q}_2, T_2) = L_{20} + L_{2z}e^{-a_2(h-2r-z)} \end{aligned} \quad (7)$$

Where L_{*0} are the inductances when no objects are present in the magnetic field volume, while L_{*z} and a_* are coefficients that take into account the variation of the inductance due to the presence of the ball in the magnetic field.

Equations of motion To derive the equations of motion of the system, we can substitute the kinetic, dissipated, and potential energy terms into the Lagrange's equation 1. Notice that by analyzing the system, we can see that the generalized coordinates are z , q_1 , and q_2 , and so the vector of generalized coordinates is $\mathbf{u} = [z, q_1, q_2]^T$.

Once \mathbf{u} has been identified, the procedure to derive the equations of motion is straightforward. Following Equation 1, we can write the following system of equations:

$$\begin{cases} \frac{d}{dt} \left(\frac{\partial \mathcal{T}}{\partial \dot{z}} \right) - \frac{\partial \mathcal{T}}{\partial z} + \frac{\partial \mathcal{D}}{\partial \dot{z}} + \frac{\partial \mathcal{U}}{\partial z} = \mathcal{Q} \\ \frac{d}{dt} \left(\frac{\partial \mathcal{T}}{\partial \dot{q}_1} \right) - \frac{\partial \mathcal{T}}{\partial q_1} + \frac{\partial \mathcal{D}}{\partial \dot{q}_1} + \frac{\partial \mathcal{U}}{\partial q_1} = \mathcal{Q} \\ \frac{d}{dt} \left(\frac{\partial \mathcal{T}}{\partial \dot{q}_2} \right) - \frac{\partial \mathcal{T}}{\partial q_2} + \frac{\partial \mathcal{D}}{\partial \dot{q}_2} + \frac{\partial \mathcal{U}}{\partial q_2} = \mathcal{Q} \end{cases} \quad (8)$$

By substituting the energetic terms obtained in Equations 2, 3, 4, 5 into the set of equations above, we obtain the following equations of motion:

$$\begin{cases} m\ddot{z} - \frac{1}{2} \frac{\partial L_1}{\partial z} \dot{q}_1^2 - \frac{1}{2} \frac{\partial L_2}{\partial z} \dot{q}_2^2 + \frac{1}{2} C_d A \rho \dot{z}^2 - mg = 0 \\ L_1 \ddot{q}_1 + \frac{\partial L_1}{\partial z} \dot{z} \dot{q}_1 + R_1 \dot{q}_1 - V_1 = 0 \\ L_2 \ddot{q}_2 + \frac{\partial L_2}{\partial z} \dot{z} \dot{q}_2 + R_2 \dot{q}_2 - V_2 = 0 \end{cases} \quad (9)$$

For convenience, we can transform the second order differential equations into first order differential equations by introducing a fourth equation in the set above and considering the currents as state variables.

$$\begin{cases} \dot{z} = v \\ \dot{v} = m^{-1} \left(\frac{1}{2} \frac{\partial L_1}{\partial z} I_1^2 + \frac{1}{2} \frac{\partial L_2}{\partial z} I_2^2 - \frac{1}{2} C_d A \rho \dot{z}^2 + mg \right) \\ \dot{I}_1 = L_1^{-1} \left(-\frac{\partial L_1}{\partial z} \dot{z} I_1 - R_1 I_1 + V_1 \right) \\ \dot{I}_2 = L_2^{-1} \left(-\frac{\partial L_2}{\partial z} \dot{z} I_2 - R_2 I_2 + V_2 \right) \end{cases} \quad (10)$$

The set of equations above represents the complete mathematical model of the MLS system. One can notice that the equations are both nonlinear and coupled, making the system hard to analyze and control.

Neglecting velocity terms In the optics of simplifying the model and making it easier to analyze and control, we can neglect all the terms in Equation 10 that are linearly dependent on the velocity of the ball. This assumption is reasonable due to the fact that the velocity of the ball (as also reported in later section of the report) will never be greater than a few centimeters per second. This means that, considering $\dot{z} \approx 10[mm/s]$, we can write the following inequality:

$$\begin{aligned} \left| -\frac{1}{2} C_d A \rho \dot{z}^2 \right| &<< mg \\ \left| -\frac{\partial L_1}{\partial z} \dot{z} I_1 \right| &<< V_1 \\ \left| -\frac{\partial L_2}{\partial z} \dot{z} I_2 \right| &<< V_2 \end{aligned} \quad (11)$$

By doing so, we can simplify the equations of motion as:

$$\begin{cases} \dot{z} = v \\ \dot{v} = m^{-1} \left(\frac{1}{2} \frac{\partial L_1}{\partial z} I_1^2 + \frac{1}{2} \frac{\partial L_2}{\partial z} I_2^2 + mg \right) \\ \dot{I}_1 = L_1^{-1} (-R_1 I_1 + V_1) \\ \dot{I}_2 = L_2^{-1} (-R_2 I_2 + V_2) \end{cases} \quad (12)$$

2.1.2 Black zone control

A final important remark has to be made about the so-called *black zone* of the system, that are the regions where the current flowing through the coils is no more reachable.

In particular, by simply connect the power supply to the coils, a minimum voltage will be applied and a certain amount of current will flow through the coils. In the following, we will refer to this current and voltage as I_{*min} and V_{*min} respectively.

Because of this, the above derived model must be slightly modified to take into account the black zone of the system.

In particular, the set of Equations 12 can be rewritten as:

$$\begin{cases} \dot{z} = v \\ \dot{v} = m^{-1} \left(\frac{1}{2} \frac{\partial L_1}{\partial z} I_1^2 + \frac{1}{2} \frac{\partial L_2}{\partial z} I_2^2 + mg \right) \\ \dot{I}_1 = L_1^{-1} (-R_1 I_1 + V_1 + R_1 I_{1min}) \\ \dot{I}_2 = L_2^{-1} (-R_2 I_2 + V_2 + R_2 I_{2min}) \end{cases} \quad (13)$$

2.1.3 Literature model

To be fixed and adjusted.

In the literature, the model of the MLS system is often further simplified by considering empirical values associated with the inductances and resistances of the coils. In particular, from the **Inteco** manual, the following set of equations is reported:

$$\begin{cases} \dot{z} = v \\ \dot{v} = m^{-1} \left(\frac{1}{2} \frac{\partial L_1}{\partial z} I_1^2 + \frac{1}{2} \frac{\partial L_2}{\partial z} I_2^2 + mg \right) \\ \dot{I}_1 = \frac{1}{f_1(z)} (-I_1 + kiU_1 + ci) \\ \dot{I}_2 = \frac{1}{f_2(z)} (-I_2 + kiU_2 + ci) \end{cases} \quad (14)$$

Where $f_1(z)$ and $f_2(z)$ are empirical functions that take into account the variation of the inductances due to the presence of the ball in the magnetic field and have the following form:

$$\begin{aligned} f_1(z) &= \frac{f_{IP1}}{f_{IP2}} e\left(-\frac{z}{f_{IP2}}\right) \\ f_2(z) &= \frac{f_{IP1}}{f_{IP2}} e\left(-\frac{h-2r-z}{f_{IP2}}\right) \end{aligned} \quad (15)$$

2.2 Model Linearization

The model derived in the previous subsection is highly non-linear. In order to begin able to apply linear control techniques, it is necessary to linearize the model around a given operating point.

From now on, we will suppose the operating point as:

$$\mathbf{x}_{op} = \begin{bmatrix} x_{op} \\ v_{op} = 0 \\ I_{1op} \\ I_{2op} \end{bmatrix} \quad (16)$$

By doing so, the linearized model can be obtained by performing a Taylor expansion up to the first order terms of the non-linear model (Equations 13 or Equations 14) around the operating point.

Before performing the linearization, we briefly recall the general form of a Taylor expansion of a function $f(\mathbf{x})$ around a point \mathbf{x}_{op} :

$$f(\mathbf{x}) \approx f(\mathbf{x}_{op}) + \nabla f(\mathbf{x}_{op}) \cdot (\mathbf{x} - \mathbf{x}_{op}) \quad (17)$$

Where $\nabla f(\mathbf{x}_{op})$ is the gradient of $f(\mathbf{x})$ evaluated at \mathbf{x}_{op} .

By applying the Taylor expansion to the non-linear model, the linearized model can be obtained as:

$$\dot{\mathbf{x}} \approx \mathbf{f}(\mathbf{x}_{op}) + \left. \frac{\partial \mathbf{f}}{\partial \mathbf{x}} \right|_{\mathbf{x}_{op}} \cdot (\mathbf{x} - \mathbf{x}_{op}) \quad (18)$$

Considering now the set of Equations 13, the linearized model can be obtained as:

2.3 State Space Representation

The linearization of the system is done by computing the Jacobian matrix of the system around the desired operating point.

At the end of the process, we obtain the state space representation of the system:

$$\begin{cases} \dot{\mathbf{x}} = A\mathbf{x} + B\mathbf{u} \\ y = C\mathbf{x} \end{cases} \quad (19)$$

We can define the state vector \mathbf{x} and the input vector \mathbf{u} as:

$$\mathbf{x} = \begin{bmatrix} z \\ v \\ I_1 \\ I_2 \end{bmatrix} \quad \mathbf{u} = \begin{bmatrix} 0 \\ 0 \\ V_1 \\ V_2 \end{bmatrix} \quad (20)$$

The matrices A , B and C are then defined as:

$$A = \begin{bmatrix} ? & ? & ? & ? \\ ? & ? & ? & ? \\ ? & ? & ? & ? \\ ? & ? & ? & ? \end{bmatrix} \quad B = \begin{bmatrix} 0 \\ 0 \\ ? \\ ? \end{bmatrix} \quad C = [1 \quad 0 \quad 0 \quad 0] \quad (21)$$

2.4 Parameters identification

In order to control the system, we need to identify its parameters. To do so, different tests type will be performed, such as:

1. **Direct Measurement:** The first step is to measure all the quantity of the system that can be directly measured or retrieved from well established literature.
2. **RL Circuit Identification:** The second step is to identify the parameters of the RL circuit. This will be done by applying a step input to the system and measuring the current;
3. **Characterization of ball influence:** The last step is to identify how the presence of the ball affects the coils and the magnetic field. This will be done by measuring the inductance of the coils with the ball positioned at different heights.

All the above tests that involve any kind of measurement from the system will be performed leveraging the data acquisition system included in the **Inteco** control unit.

Based on the mathematical model developed in Section 2.1 and the set of Equations 13 and Equations 14, the following parameters need to be identified:

Name	Description	Unit	Test #
m	Mass of the ball	kg	1
r	Radius of the ball	m	1
H	Distance between the two coils	m	1
C_d	Drag coefficient	$N \cdot s/m$	1
ρ	Density of the air	kg/m^3	1
L_{*0}	Static inductance of the coils	H	2
L_{*z} & a_*	Dynamic inductance characteristics	H & $1/m$	3
R_{*0}	Static resistance of the coils	Ω	2
f_{IP1}	Empirical parameters	$m \cdot s$	1
f_{IP2}	Empirical parameters	m	1
I_{*min}	Minimum current	A	2
I_{*max}	Maximum current	A	2
V_{*min}	Minimum voltage	V	2
V_{*max}	Maximum voltage	V	2

Table 1: Parameters to be identified

Notice that column **Test #** in Table 1 refers to the test ID in the list above.

Direct Measurement The mass of the ball and its radius can be directly measured using a scale and a caliper, respectively. Also the distance between the two coils can be measured using a caliper.

The drag coefficient can be obtained from well established literature. In the following, we will use the drag coefficient of a sphere in a fluid and we will assume it to be constant for all the range of velocities we are going to work with. This, for relatively low velocities, can be considered a good approximation.

The density of the air can be obtained from well established literature.

By doing so, we will have the following values:

Parameter	Value
m	$0.06157 kg$
r	$0.06125/2 m$
H	$0.098 m$
C_d	$0.45 N \cdot s/m$
ρ	$1.21 kg/m^3$

Table 2: Directly measured parameters

RL Circuit Identification The RL circuit identification will be done by applying a step input to the system and measuring the current. The current will be measured using the data acquisition system included in the **Inteco** control unit.

The identification will be done by fitting the measured current to the following model:

$$i(t) = \frac{V_{*max}}{R_{*0}} \left(1 - e^{-\frac{R_{*0}}{L_{*0}}t} \right) \quad (22)$$

Also the minimum and maximum current and voltage can be measured directly using the data acquisition system.

In Figure 4 we can see 10 transient responses of the current in the RL circuit (black dashed lines) as well as the fitted model (red solid line).

Figure 4: RL circuit identification

By doing so, we will have the following values:

Parameter	Value
L_{*0}	? H
R_{*0}	? Ω
I_{*min}	? A
I_{*max}	? A
V_{*min}	? V
V_{*max}	? V

Table 3: RL circuit identification parameters

Characterization of ball influence The characterization of the ball influence will be done by measuring the inductance of the coils with the ball positioned at different heights.

For convenience and time saving, we will adopt a different strategy that will allow us to measure directly the sensitivity of the inductance to the ball position. To do so, we recall Equation ?? and in particular the equation relative to \dot{v} :

$$\dot{v} = m^{-1} \left(\frac{1}{2} \frac{\partial L_1}{\partial z} I_1^2 + \frac{1}{2} \frac{\partial L_2}{\partial z} I_2^2 - \frac{1}{2} C_d A \rho \dot{z}^2 + mg \right) \quad (23)$$

If we consider the system at rest, we can simplify the equation as follows:

$$0 = \frac{1}{2} \frac{\partial L_1}{\partial z} I_1^2 + \frac{1}{2} \frac{\partial L_2}{\partial z} I_2^2 + mg \quad (24)$$

Supposing now that only the first coil is energized, we can further simplify the equation as follows:

$$0 = \frac{1}{2} \frac{\partial L_1}{\partial z} I_1^2 + mg \quad (25)$$

Which leads to:

$$\frac{\partial L_1}{\partial z} = -2 \frac{mg}{I_1^2} \quad (26)$$

This last equation basically tells us that in steady state conditions, when the ball is levitating (i.e. $\dot{z} = 0$ and not supported by any platform), the sensitivity of the inductance of the first coil has an analytical expression that can be directly measured by measuring the current in the first coil.

In order to follow this approach, a linearly increasing voltage has been applied to the first coil and the current corresponding to the levitation of the ball has been measured.

In Figure 5 we can see both the position of the ball and the current circulating in the first coil. By indentifying the current at which the ball starts to levitate (i.e. the ball starts to move upwards), we can than use Equation 26 to identify the dynamic inductance characteristics.

Figure 5: Levitation current

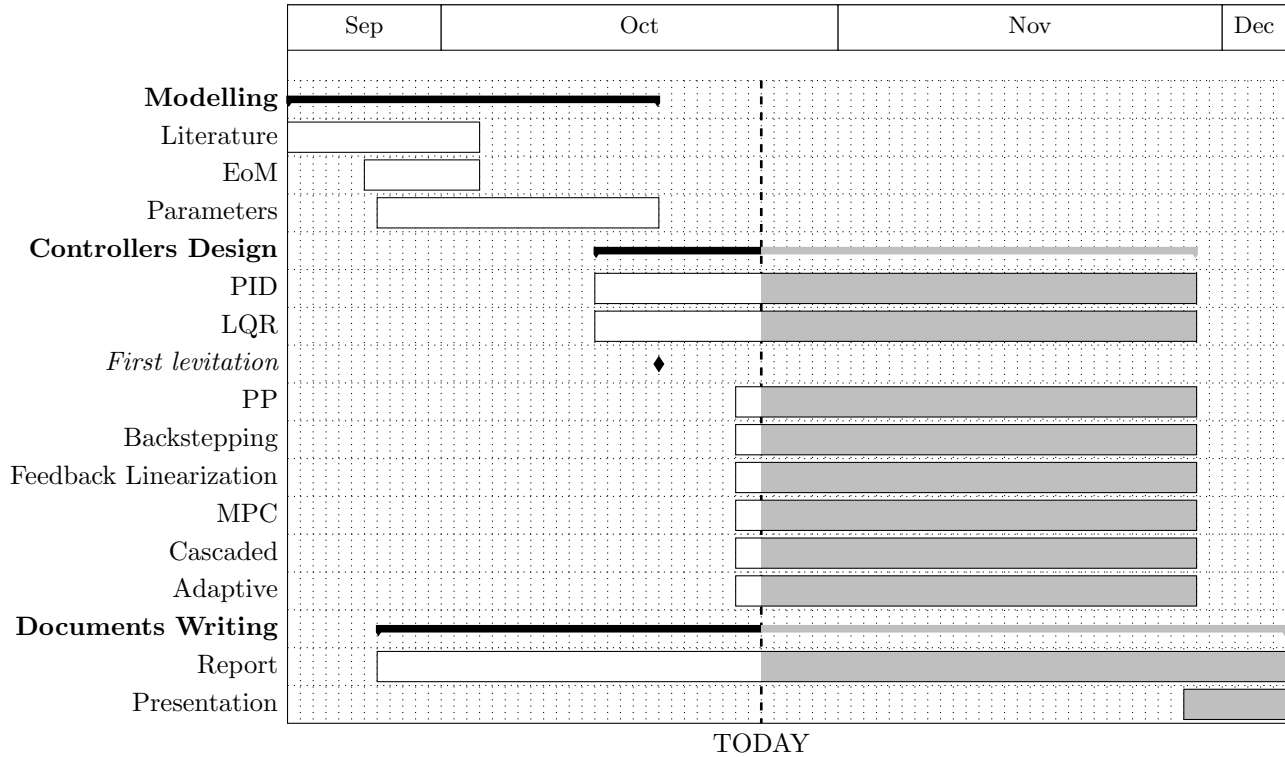
The test described above has been repeated for different heights of the ball, in order to fully characterize the dynamic inductance characteristics over the range of possible ball positions. The results are shown in Table 4 and in Figure 6.

Position (z) [mm]	Current (I) [A]	Control Voltage (V) [V]	Sensitivity ($\partial L/\partial z$) [H/m]
0.0	0.0	0.0	0.0
0.0	0.0	0.0	0.0

Table 4: Dynamic inductance characteristics

Figure 6: Dynamic inductance characteristics

3 Controller Design



Bocchio	Daniele	Sara
Backstepping	MPC	PID
Feedback Linearization	Cascaded	LQR
	Adaptive / Swarm	Pole Placement

Table 5: Controllers assignment

Note 1: When applicable, one should also design/implement/associate the following ‘logics’:

- Anti windup;
- Gain scheduling <https://www.youtube.com/watch?v=g7R1USqJ0Uo>;
- Kalman Filter;
- Other, search online.

To see if one of the above logics is applicable, search for the theoretical assumptions & hypothesis that the logic is based on. Of course, if the assumptions are not met the logic is not applicable.

Note 2: Discretize whatever you design.

Looks like Simulink and MagLev have been designed so to ‘automatically discretize’ the controllers. However, I suspect that when we run a continuously designed controller on the MagLev, all the calculations are performed by Simulink and my poor PC and not the yellow power supply of the MagLev.

Basically, if Marconi discovers that we haven’t discretized anything, we are screwed.

3.1 PID Controller

The Proportional-Integral-Derivative (PID) controller is a simple controller that uses the error signal, its history and its derivative to compute the control signal. It is a widely used controller in industry due to its simplicity and effectiveness in many applications.

$$u(t) = K_p e(t) + K_i \int_0^t e(\tau) dt + K_d \frac{de(t)}{dt} = K_p \left(e(t) + \frac{1}{T_i} \int_0^t e(\tau) dt + T_d \frac{de(t)}{dt} \right) \quad (27)$$

Where K_p , K_i and K_d are the proportional, integral and derivative gains, respectively, and T_i and T_d are the integral and derivative time constants, respectively.

3.1.1 Simple PID

Bla bla.

3.1.2 PID with Anti-Windup correction

Bla bla.

3.1.3 Bla bla bla

3.2 Cascaded Controller

3.3 Pole Placement Controller

3.4 LQR Controller

3.5 MPC Controller

3.6 Adaptive Control

3.7 Backstepping

3.8 Feedback Linearization

4 Controllers Comparison

5 Conclusions

References

- [1] Wikipedia contributors. Scmaglev — Wikipedia, the free encyclopedia. <https://en.wikipedia.org/w/index.php?title=SCMaglev&oldid=1243224393>, 2024. [Online; accessed 28-September-2024].